Determination of Site Amplification in East-Central Iran from Inversion of Strong-Motion Records

Behzad Hassani
School of Civil Engineering, University of Tehran, Email: behhassani@gmail.com

Hamid Zafarani
Assistant Professor, International Institute of Earthquake Engineering and Seismology *(IIEES)*

Jamshid Farjoodi
Assistant Professor, School of Civil Engineering, University of Tehran

SUMMARY:
The site response of strong-motion in the East-Central Iran is determined using the generalized-inverse method of Andrews (1986). Site-amplification estimates are determined at 42 strong-motion sites that provided horizontal-component records from 40 earthquakes of magnitude M3.5 to M7.3 in the region. The inverse problem was solved in 20 logarithmically equally spaced points in the frequency band from 0.4 to 15 Hz. To obtain a unique inverse solution, a frequency-dependent site amplification as a constraint was imposed to two reference site responses. Furthermore, average site response values were correlated to the average shear wave velocity in the uppermost 30m, in high and low frequency bands. The peak frequencies of site amplifications estimated by generalized inversion method were coincided with those of horizontal to vertical (H/V) spectral ratios for the S-wave portion of records. However, due to the shortcomings of the H/V ratio technique, a perfect matching in amplitude was not obtained.

Kywords: Generalized inversion; Site response; East-Central Iran

1. INTRODUCTION

Ground motion at a particular site is influenced by source, path and site effects. Site factors include a combination of amplification through the crustal profile and near-surface attenuation. To perform a reliable estimation of seismic hazard by using physical modeling approach, the study of region-specific source and wave propagation parameters, as well as seismic-site responses, is a priority for research. In this study for estimating seismic parameters, the central-east region as one of the most highly seismic zones in Iran, is selected. The generalized inversion of the S-wave amplitude spectra from the strong-motion network data in the East-Central region of Iran is used to estimate source, site and path effects. This technique was first presented by Andrews (1986) by recasting the method of spectral ratios into a generalized inverse problem. Since after, the approach has been used and developed by numerous authors. In the following, we report the results obtained on site response in the above area.

By gathering events, in a long period of time, form 1979 to 2007, almost all of significant earthquakes in the region were selected for the analysis. These earthquakes were recorded in different stations, which are located in a vast area in the East-Central region and cover a wide range of hypocentral distances. Consequently, more general attenuation parameters are obtained from selected database. The final database contains two separate areas in the desired region (Fig. 1.1 & Fig. 1.2), but in order to obtain an average estimation of attenuation parameters, both parts of the database are solved in a single system of equations.

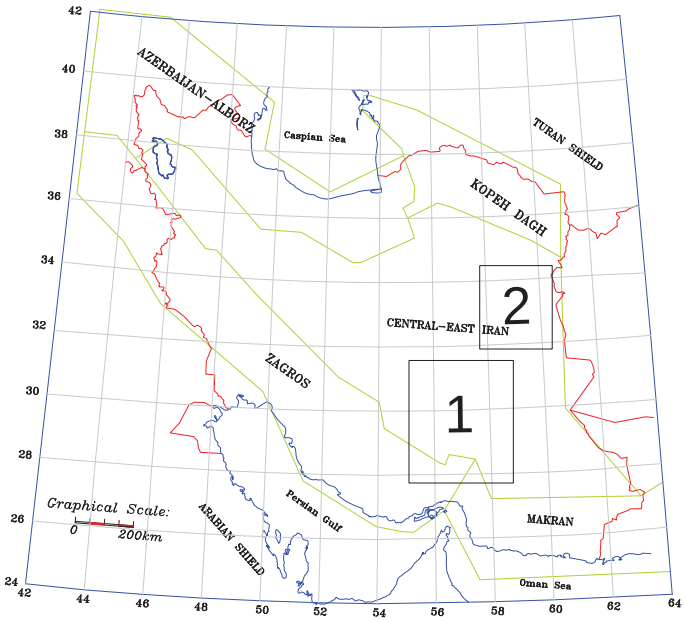

Figure 1.1. The principal seismotectonic zones of Iran according to Mirzaei et al. (1999). Two separate areas in the East-Central region, studied in this paper are also shown.

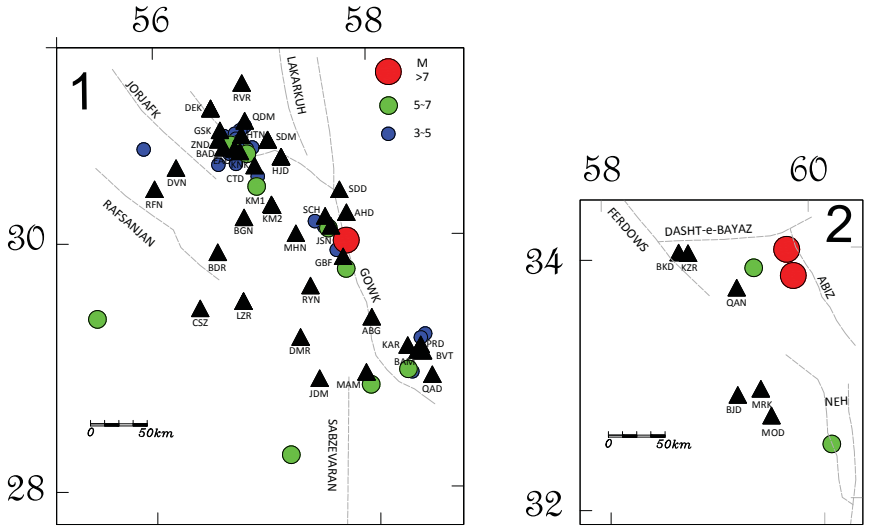

Figure. 1.2. Two separate areas in East-Central region of Iran, epicenter location of the earthquakes analyzed for the present study (circles), strong-motion stations (triangles) and active faults in each part (gray dashed-line).

2. DATABASE AND DATA PROCESSING

All of the data used in this study, were recorded by the Iranian Strong Motion Network (ISMN), which have been installed and maintained by Building and House Research Center (BHRC). Using the conventional filtering method, major proportion of analog strong motion records is felt to be too poor to be included in practical engineering applications. Using the modified wavelet de-noising method, it is possible to retrieve a large number of analog acceleration records which was not possible to correct using conventional methods of correction (Ansari et al., 2007). Multi-resolution wavelet analysis was performed here, to remove undesirable noise from the recorded signals.

To obtain the final database, following steps were performed: (1) earthquakes with reported seismic characteristics, since the start of ISMN installation up to the end of 2007, were selected in the East-Central region of Iran. (2) Correctable time series were left in the database, while others eliminated. (3) Three-component records with only one correctable horizontal component were excluded from the database. (4) Earthquakes with at least three and stations with at least two records, which are linked to the reference sites, compose the final database. Following these steps, the final database contains data from 196 records of 40 earthquakes with magnitude ranging from M 3.5 to M 7.3 and with focal depths from 3 to 20 km. These data were recorded in 42 strong-motion stations at hypocentral distances ranging from 9 to 200 Km. Finally, earthquake epicenters and recording stations, were located in two separate areas (1 and 2; shown in Fig. 1.2).

Since the major portion of the seismic energy is generated in the form of S-waves, the analysis should be performed on this part of the strong motion records. The onset of the S-wave arrival time (t_1) was estimated by the Husid plot of energy buildup. In this approach the time equivalent of 5 percent of energy plot is assumed as t_1. Also for estimating the time of the last arrival of the direct S-wave (t_2), cumulative root mean square (RMS) function was used. In this technique, t_2 is determined as the point where the cumulative RMS function starts decreasing along the time axis. After estimating t_1 and t_2, a cosine taper was applied at the beginning and end of each window. The length of each of these tapers will be 5 percent of the total trace length. Fast Fourier Transform (FFT) was used to calculate Fourier amplitude spectrum. The spectrum was smoothed using a 5 point moving average filter, and interpolated at 20 points, which are equally spaced on the logarithmic scale, between 0.4 and 15 Hz. A sample record of the database is used to demonstrate the approach used in this study for finding t_1 and t_2. The horizontal motion spectra (Fourier amplitude) were computed as the resultant geometric mean of the orthogonal components of motion.

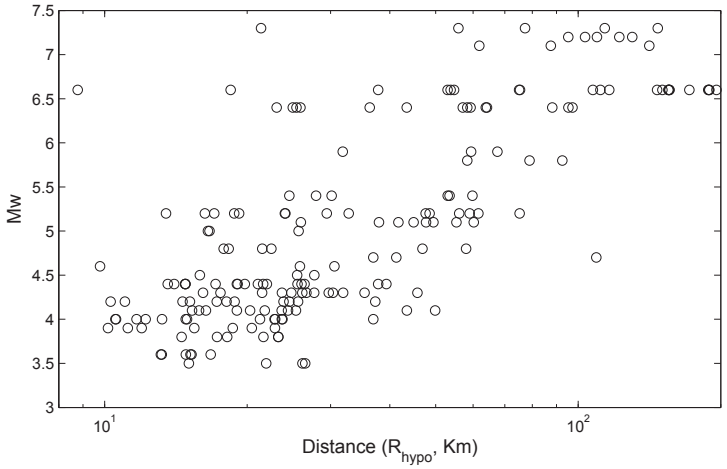

Figure 2.1. Magnitude-distance distribution of records used in this study

3. GENERALIZED INVERSION

Andrews (1986) recast the method of spectral ratios into a generalized-inverse problem by simultaneously solving the data of multiply recorded events in terms of site effect, source term, and quality factor. The most widely accepted formulation of the ground-motion spectrum was used in this study (see Eqn. 3.1). This general representation of the problem implicitly accepts the validity of the principle of superposition, which means each of source, site and path effects, can be considered as a separate filter. Suppose the database contains of J sites over which I events have been recorded. Then the Fourier amplitude spectrum of the ith event recorded at the jth site $Y_{ij}(f)$ can be written in the frequency domain as a product of a source term $E_i(f)$; a path term $P_{ij}(f, R)$; and a site-effect term $G_j(f)$.

$$Y_{ij}(f) = E_i(f) \times P_{ij}(f,R) \times G_j(f) \tag{3.1}$$

A path effect term $P_{ij}(f,R)$ representing geometric and anelastic attenuation is given by:

$$P_{ij}(f,R) = Z(R_{ij}).\exp\left(\frac{-pfR_{ij}}{Q_s(f).b_s}\right) \tag{3.2}$$

Where R_{ij} is the hypocentral distance between the *i*th event and the *j*th station, $Z(R_{ij})$ represents attenuation due to geometrical spreading, $Q_S(f)$ and β_S are S-wave frequency dependent quality factor and velocity, respectively. A site effect $G_j(f)$ representing site amplification and the diminution function (path-independent loss of energy) was also considered:

$$G_j(f) = A_j(f) \times \exp(-pk_0 f) \tag{3.3}$$

where $A_j(f)$ is the *j*th station amplification function and κ_0 represents the diminution parameter or zero-distance kappa factor (Anderson & Hough, 1984). Substituting Eqn. 3.2. and 3.3. into 3.1., and performing a logarithmic operation on the resulting equation, we have the following result

$$\begin{aligned} &s_{ij}(f) \times (\ln(Y_{ij}(f)) + pk_0 f - \ln(Z(R_{ij}))) = \\ &- s_{ij}(f) \times (pfR_{ij} / b_s) \times Q_s^{-1}(f) + s_{ij}(f) \times \ln(E_i(f)) + s_{ij}(f) \times \ln(A_j(f)) \end{aligned} \tag{3.4}$$

or

$$d_{ij}(f) = g_{ij}(f) Q_s^{-1}(f) + s_{ij}(f).\ln(E_i(f)) + s_{ij}(f).\ln(A_j(f)) \tag{3.5}$$

where $d_{ij}(f) = s_{ij}(f) \times (\ln(Y_{ij}(f)) + pk_0 f - \ln(Z(R_{ij})))$, $g_{ij}(f) = -s_{ij}(f) \times (pfR_{ij} / b_s)$ and $s_{ij}(f)$ denotes a frequency-dependent weighted factor that balances the quality of the database.

If we consider a total number of recordings *N*, corresponding to a number of earthquakes *I* recorded at a total number of stations *J*, then a compact matrix formulation for Eqn. 3.5. can be represented in the following manner:

$$[Y] = [A][X] \tag{3.6}$$

where $[Y]$ represents a vector containing the ground motion amplitude corrected by the geometrical spreading and the diminution function and each member of it represents a vector with n rows, when *n* is the number of selected points in desired frequency range; $[A]$ denotes a sparse matrix containing only three nonzero elements in each row (from row 1 to row N). The first column contains a non-zero vector with n rows while other columns represent an $n \times n$ diagonal matrix. $[X]$ denotes a matrix holding $I + J + 1$ unknown terms, namely, the vector solution containing the inverse of quality factor $Q_S^{-1}(f)$, the source effect $\ln(E_i(f))$ and the site effect $\ln(A_j(f))$ when each of its members represents a vector with n rows. As described before, the database contains two separated zones in the East-Central region. In order to solve the undetermined degree of freedom in this set of equations, a reference site was considered in each part, consequently, this formulation yields $(N + 2) \times n$ equations.

The over-determined system of linear equations given by Eqn. 3.6. doesn't have a unique solution, although we can find its optimal least-square solution using following equation,

$$X = ([A]^T [A])^{-1} [A]^T Y \tag{3.7}$$

where the T and -1 exponents indicate transpose and inverse operation respectively.

4. SITE RESPONSES

Applying the inversion method to the selected database, the source spectra, site responses and S-wave quality factors were obtained simultaneously. In this study just the site response results are discussed and the other parameters will be discussed in additional papers.

The site amplification ($A_j(f)$) for 42 stations is the outcome of this study which was obtained in the defined frequency range, using generalized inversion method. Solid line in Fig. 4.1. represents the site amplification factors estimated from generalized inversion at each station. Furthermore, the name, number of records, geographic coordinates, three-letter abbreviation, maximum response, fundamental frequency and the average velocity of shear waves in the top 30 m (β_{30}) corresponding to each station are presented in Table. 4.1.

To compare the results of this method with earthquake H/V method of Lermo and Chávez-García (1993), the results of H/V method are also shown in Dashed lines, besides the gray area represents one standard deviation corresponding to generalized inversion method. The H/V method assumes that the local site conditions do not significantly influence the vertical component of the ground motion and the H/V spectral ratios may be used as an indicator of site effects. Previous studies have shown that the H/V method is consistent with the general geological conditions of the recording sites and it is capable of revealing the predominant frequency peaks. However, the general conclusion is that the technique fails in amplitude level, especially for higher modes (Sokolov et al., 2007). In Fig. 4.1., QAN and CTD are the reference sites; thus, the site amplification factor at these sites was set to be equal to the predetermined generic rock site amplification of Boore and Joyner (1997). The H/V ratios of these sites also confirm our decision to select them as reference sites.

In Fig. 4.1., generally, comparison of H/V results with the inversion technique reveals that both methods practically represent the same shape of site spectra, but the average of site amplification factors estimated from the generalized inversion scheme, is generally less than the H/V method.

The site response values yielded by each of the above two methods (inversion and H/V) were averaged in the selected frequency band of this study. The result of the comparison between inversion results versus H/V is shown in Fig. 4.2. The comparison of site response values of inversion and those of H/V shows a relatively large scatter and lower H/V values than those yielded by the inversion method. Similar results for other seismogenic zones have been reported (Salzar et al., 2007; Bonilla et al., 1997). An important consideration for interpretation of these results is the adequacy of the average velocity of shear waves in the top 30 m of soil, to soil or rock classification.

The average shear-wave velocity to a depth of 30 m β_{30} is available at 26 stations (Table. 4.1). Based on the results of Zare et al. (1999), these stations were categorized in two groups, rock (β_{30}>500 m/s) and soil (β_{30}<500 m/s). In order to typically depict the differences in the estimates of site amplifications, site amplification factors at each station were averaged over two frequency bands. A bandwidth of 2.1 Hz was used for the low-frequency band, LFB= 0.4 to 2.5 Hz, and 3.3 Hz for the high-frequency band, HFB= 3 to 6.3 Hz, with corresponding geometric central frequencies at 1 and 5 Hz, respectively. Then the averaged amplification factors (*Amp*) at each frequency bands were computed and related to the shear wave velocity in logarithmic scale (Fig. 4.3).

Using the least square fitting, the relation for the LFB can be presented as follow:

$$\ln(Amp) = (-\ 0.531 \pm\ 0.23)\ln b_{30} + (4.48 \pm\ 1.50) \tag{3.8}$$

and for the HFB can be expressed as:

$$\ln(Amp) = (-\ 0.19 \pm\ 0.25)\ln b_{30} + (2.63 \pm\ 1.63) \tag{3.9}$$

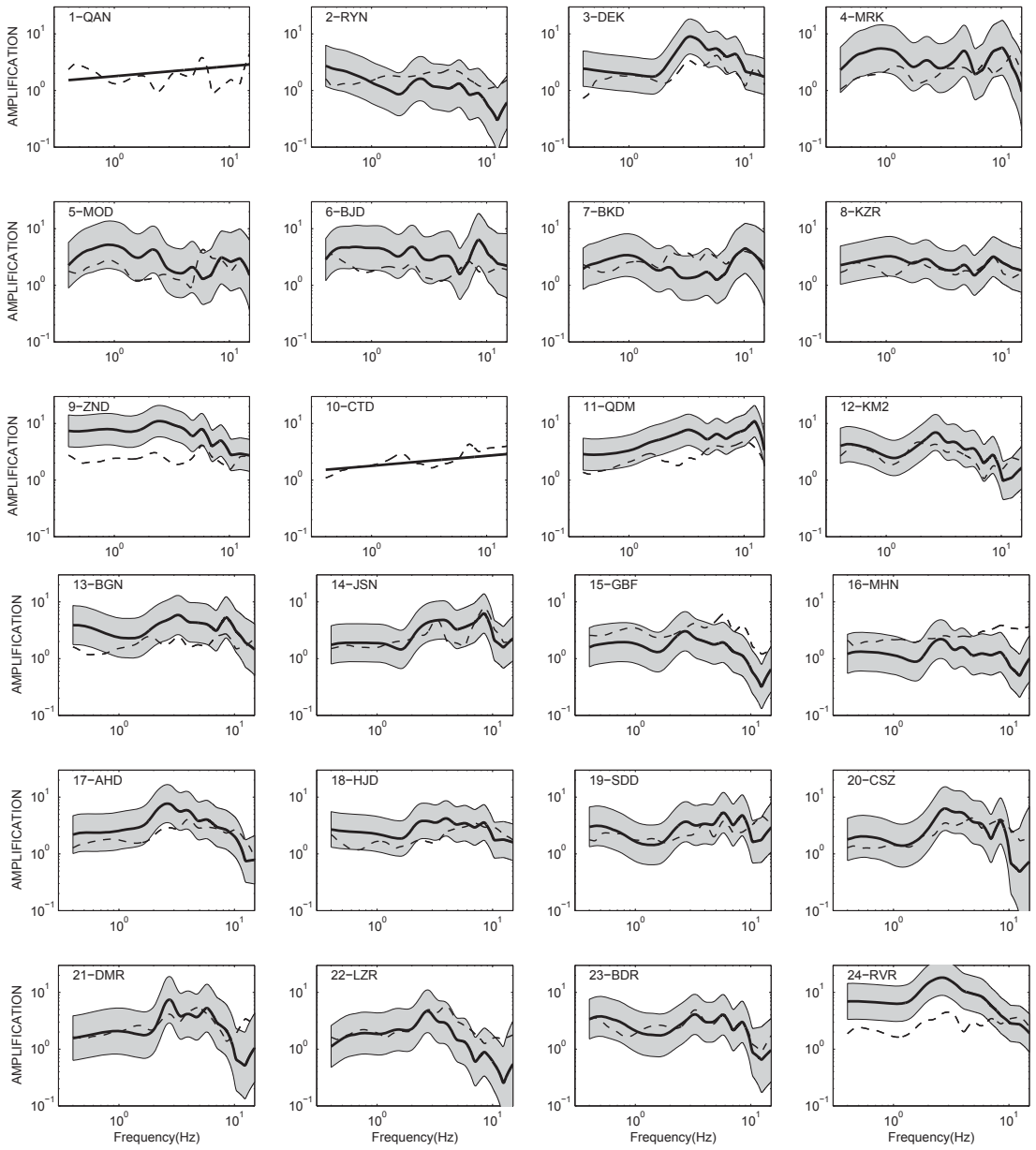

Figure 4.1. Site-amplification spectra at 24 among 42 stations obtained from performed inversion (solid), arrived from H/V method (dashed), and one standard deviation range (shaded).

Table 4.1. Stations coordinates and generalized inversion result.

St.NO	Station Name	N†	latitude (deg)	longnitude (deg)	Abbreviation	Maximum Site Response	fundamental Frequency (Hz)	β_{30}(m/sec)
1	***Qaen***	2	33.7	59.2	***QAN***	2.9	15.0	889
2	Rayen	2	29.6	57.4	RYN	2.7	0.4	544
3	Dasht-e-Khak	3	31.1	56.6	DEK	9.3	3.3	-
4	Marak	2	32.9	59.4	MRK	5.9	1.0	-
5	Mood	2	32.7	59.5	MOD	5.7	1.0	-
6	Birjand	3	32.9	59.2	BJD	6.6	8.5	525
7	Bosk Abad	2	34.0	58.7	BKD	4.5	10.2	-
8	Khezri	3	34.0	58.8	KZR	3.3	10.0	762
9	Zarand	12	30.8	56.6	ZND	11.1	2.2	226
10	***Chatrood***	6	30.6	56.9	***CTD***	2.9	15.0	852
11	Qadrooni Dam	13	31.0	56.8	QDM	11.2	12.4	-
12	Kerman 2	5	30.3	57.1	KM2	7.6	2.7	-
13	Baghin	3	30.2	56.8	BGN	6.2	3.3	516
14	Joshan	4	30.1	57.6	JSN	6.5	8.5	776
15	Golbaf	3	29.9	57.7	GBF	3.2	2.7	365
16	Mahan	4	30.1	57.3	MHN	2.3	2.7	-
17	Andoohjerd	4	30.2	57.8	AHD	8.1	2.7	566
18	Horjand	3	30.7	57.2	HJD	4.4	3.9	-
19	Shahdad	2	30.4	57.7	SDD	5.6	5.8	-
20	Cheshmeh sabz	2	29.5	56.4	CSZ	6.7	2.7	678
21	Darmazar	2	29.2	57.3	DMR	8.7	2.7	-
22	Laleh Zar	2	29.5	56.8	LZR	5.2	2.7	-
23	Bardsir	2	29.9	56.6	BDR	4.4	3.3	539
24	Ravar	3	31.3	56.8	RVR	18.8	2.7	-
25	Sirch	4	30.2	57.6	SCH	6.8	2.2	398
26	Bam	4	29.1	58.4	BAM	4.8	0.4	499
27	Mohammad Abad-M	3	28.9	57.9	MAM	4.9	2.7	507
28	Abaragh	4	29.3	57.9	ABG	4.4	15.0	-
29	Jiroft Dam1	2	28.9	57.5	JDM	3.9	2.7	-
30	Shirinrood Dam1	4	30.8	57.0	SDM	12.3	12.4	824
31	Baha Abad	11	30.7	56.6	BAD	12.3	3.9	385
32	Khanook	16	30.7	56.8	KNK	5.4	8.5	-
33	Hotkan	16	30.8	56.8	HTN	13.1	2.7	837
34	kerman1	4	30.3	57.1	KM1	7.6	0.6	-
35	Qotb Abad	3	28.9	58.5	QAD	4.1	2.7	648
36	Posht Rood	3	29.1	58.4	PRD	9.1	0.4	329
37	Khaje Asgar	2	29.1	58.3	KAR	12.3	2.7	463
38	Barvat	3	29.1	58.4	BVT	7.0	8.5	491
39	Eslam Abad	15	30.7	56.7	EAD	7.5	3.3	807
40	Davaran	2	30.6	56.2	DVN	10.0	12.4	752
41	Rafsanjan	2	30.4	56.0	RFN	12.2	2.7	418
42	Gisk	3	30.9	56.6	GSK	5.0	3.3	809

†N, Number of records

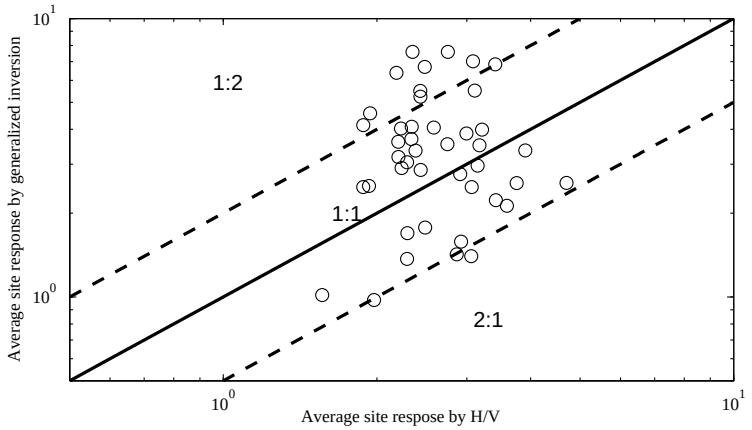

Figure 4.2. The comparison of average site response calculated by inversion versus corresponding values obtained from H/V method. The dashed lines in the figure indicate 1:2 and 2:1 lines.

It can be concluded from these two relations, that the average of the site response descends by increasing the shear wave velocity in both frequency band, and also in the LFB this reduction is more correlated to shear wave velocity in comparison with the HFB. It should be noticed that according to the shortage of geotechnical information, obtained relations have high level of uncertainties, which would be improved by further information.

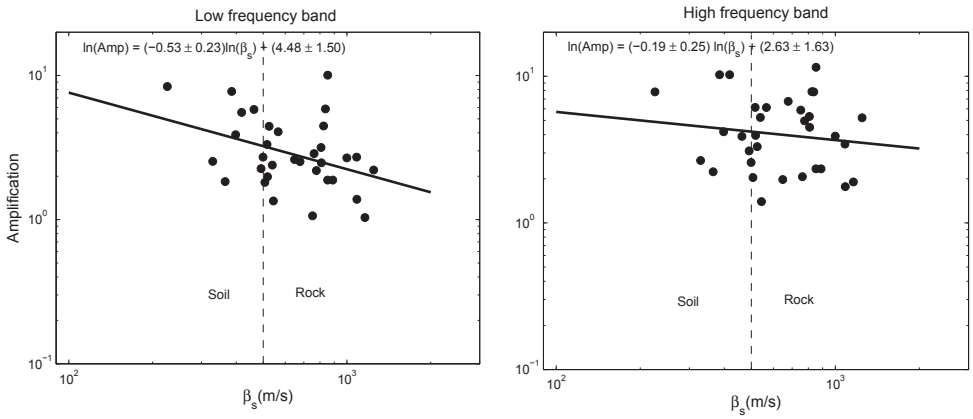

Figure 4.3. The average of site response (Amp) values at the LFB (a) and HFB (b) are plotted with respect to the average shear wave velocity of the uppermost 30m (circles). The regression line is shown by the solid line (thick). The dotted vertical line marks the transition from soil to rock as a result of Zare et al. (1999) obtained relations are also shown.

5. CONCLUSIONS

The site effects for 42 stations in East-Central Iran were obtained using generalized inversion method. The generic rock amplification of Boore and Joyner (1997) was imposed to two station in order to solve an undetermined degree of freedom in the set of equations. The site responses resulted in the current study was compared with the H/V method. Due to the shortcomings of the H/V ratio technique, we do not expect the H/V site response estimates, to perfectly match the general inversion results in amplitude, although a better match in shape was obtained and generally, comparison of results reveals that the H/V ratios successfully match the shapes of the transfer functions obtained by the inversion technique. As it can be concluded, both methods practically represent a same shape for site response spectra, but the average of values in the generalized inversion, is nearly twice the H/V method. Moreover, for two frequency bands, the average of site response spectra were computed and related to the shear wave velocity in logarithmic scale. Moreover, the site responses were averaged in two frequency bands (LFB & HFB) and correlated to β_{30}. It can be concluded that the site response descends by increasing the shear wave velocity in both frequency band, and also in the LFB this reduction is more correlated to shear wave velocity in comparison with the HFB.

ACKNOWLEDGMENT

The authors acknowledge the Building and Housing Research Centre of Iran for providing them with the accelerographic database.

REFERENCES

Anderson, J., and Hough, S. (1984). A model for the shape of the Fourier amplitude spectrum of acceleration at high frequencies. *Bulletin of the Seismological Society of America* **74**, 1969–1993.

Andrews, D. J. (1986). Objective determination of source parameters and similarity of earthquakes of different size, Earthquake Source Mechanics. *American Geophysical Union, Washington, D.C.,* 259-267.

Ansari, A., Noorzad, A. and Zare, M. (2007). Application of wavelet multi-resolution analysis for correction of seismic acceleration records. *Journal of Geophysics and Engineering* **4**, 1–16.

Bonilla, L.F., Steidl, J.H., Lindley, G.T., Tumarkin, A.G., and Archuleta, R.J. (1997), Site amplification in the San Fernando valley, California: variability of site-effect estimation using the S-wave, coda and H/V

methods. *Bulletin of the Seismological Society of America* **87**:710–30.
Boore, D.M. and Joyner, W.B. (1997), Site amplifications for Generic Rock Sites. *Bulletin of the Seismological Society of America* **87**, 327–341.
Lermo, J., and Chavez-Garcia, F. (1993). Site effect evaluation using spectral ratios with only one station. *Bulletin of the Seismological Society of America* **83**, 1574–1594.
Mirzaei, N., Mengtan, G. and Yuntai, C. (1998). Seismic source regionalization for seismic zoning of Iran: Major seismo tectonic provinces. *Earthquake Prediction Research* **7**, 465–95.
Salazar, W., Sardina, V., and Cortina, J.de. (2007). A Hybrid Inversion Technique for the Evaluation of Source, Path, and Site Effects Employing S-Wave Spectra for Subduction and Upper-Crustal Earthquakes in El Salvador. *Bulletin of the Seismological Society of America* **97**, 208–221.
Sokolov, V.Y., Loh, C.H., and Jean, W.Y. (2007). Application of horizontal-to-vertical (H/V) Fourier spectral ratio for analysis of site effect on rock (NEHRP-class B) sites in Taiwan. *Soil Dynamics and Earthquake Engineering* **27**, 314–323
Zare´, M., Bard, P.Y., Ghafory-Ashtiany, M. (1999). Site characterizations for the Iranian strong motion network. *Soil Dynamic and Earthquake Engineering* **18**:101–121.